
Latent Gaussian process with composite likelihoods for data-driven disease stratification

Siddharth Ramchandran^{1*}

Miika Koskinen^{2,3*}

Harri Lähdesmäki^{1*}

¹Dept. of Computer Science, Aalto University, Finland

²Helsinki Biobank, HUS Helsinki University Hospital, Finland

³Faculty of Medicine, University of Helsinki, Finland

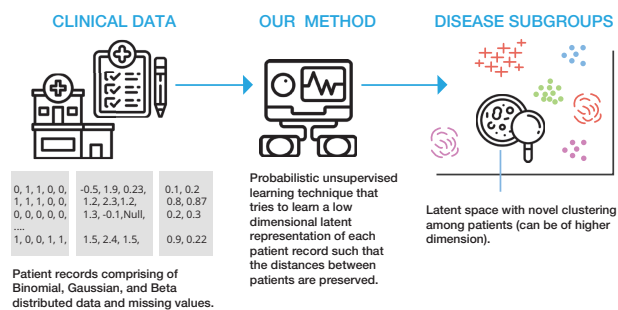
Abstract

Data-driven techniques for identifying disease subtypes using medical records can greatly benefit the management of patients' health and unravel the underpinnings of diseases. Clinical patient records are typically collected from disparate sources and result in high-dimensional data comprising of multiple likelihoods with noisy and missing values. Probabilistic methods capable of analysing large-scale patient records have a central role in biomedical research and are expected to become even more important when data-driven personalised medicine will be established in clinical practise. In this work we propose an unsupervised, generative model that can identify clustering among patients in a latent space while making use of all available data (i.e. in a heterogeneous data setting with noisy and missing values). We make use of the Gaussian process latent variable models (GPLVM) and deep neural networks to create a non-linear dimensionality reduction technique for heterogeneous data. The effectiveness of our model is demonstrated on clinical data of Parkinson's disease patients treated at the HUS Helsinki University Hospital. We demonstrate sub-groups from the heterogeneous patient data, evaluate the robustness of the findings, and interpret cluster characteristics.

1 Introduction

Personalised medicine focuses on clinical and biological characteristics of a person to optimise prediction, prevention, and treatment of diseases based on individual traits (Achenbach *et al.*, 2004; Harvey *et al.*, 2012). Diseases, such as diabetes or Parkinson's disease, manifest heterogeneous clinical symptoms that may largely vary between patients. With these diseases, for example, two or more subtypes have been identified with differing course, prognosis and genetic associations between the subtypes (Ahlqvist *et al.*, 2018; Kalia and Lang, 2015). Thus, patient stratification based on a rich dataset of clinical and biological variables with proper statistical modelling has the potential to provide insights into the underlying disease mechanism, diagnosis and therapy.

In data-driven patient stratification, cluster analysis has a vital role. For example, Ahlqvist *et al.* (2018) selected a few variables in a diabetes cohort and utilised k-means and hierarchical clustering techniques to find subgroups of patients that show similar characteristics within the clusters. Different progression patterns and risks of diabetic complications were found between the clusters.



Preprint. Under review.

*Correspondence to: siddharth.ramchandran@aalto.fi,
miika.koskinen@hus.fi, harri.lahdesmaki@aalto.fi

Figure 1: An overview of our unsupervised, generative model for disease stratification.

Another approach to achieve disease stratification is to obtain a low-dimensional representation which reveals some latent structure in the data. For originally high-dimensional data, a low-dimensional representation is also useful for visualisation purposes. Real-world patient records comprise of heterogeneous, high-dimensional data from several disparate sources. In a statistical setting, these disparate observation spaces can be represented by different likelihoods and may correspond to disease codes, procedures, laboratory measurements, medications, etc.

In this study, we aim to identify disease subtypes utilising heterogeneous patient records comprising of multiple likelihoods as well as noisy and missing data by embedding high-dimensional observations or feature vectors into a low-dimensional space while capturing the similarity between the observations. We show that incorporating all the covariates through the use of a composite likelihood constitutes a rigorous statistical model and yields promising results. Our method is summarised in Fig. 1.

Principle component analysis (PCA) is one of the most popular techniques for dimensionality reduction. The probabilistic reformulation of PCA, probabilistic principal component analysis, proposed by [Tipping and Bishop \(1999\)](#) incorporates a probabilistic model and arrives at a linear projection after the maximisation of the likelihood. Gaussian process (GP) models can powerfully perform tasks such as classification and regression and are popular algorithms in machine learning ([Rasmussen, 2004](#)). [Lawrence \(2004\)](#) reinterpreted PCA as a GP mapping from the latent space to the data space and proposed a generalisation by using a prior that allows for non-linear processes. This is called the Gaussian process latent variable model (GPLVM). In short, the GPLVM attempts to learn a smooth mapping from the latent space to the data space.

To accurately capture the latent manifold structure of the data, it is important for a dimensionality reduction algorithm to balance between preserving the distance between nearby data points and ensuring that data points that are distant in the data space are not nearby in the latent space (dissimilarity). However, the GPLVM algorithm only guarantees the latter and does not have any constraint that ensures the former. [Lawrence and Quiñonero-Candela \(2006\)](#) discusses this issue in detail and introduces the idea of incorporating a local-distance preserving constraint thereby formulating a back-constrained GPLVM. We impose this constraint using recognition models (or neural networks) which introduces a mapping from data space to latent space ([Bui and Turner, 2015](#)). The recognition models also allows for the introduc-

tion of efficient mini-batching to the optimisation of the GPLVM. To summarise, we have two models: the recognition model that preserves local distances and the probabilistic GPLVM model that preserves the dissimilarities.

GPLVMs are targeted towards homogeneous datasets (i.e. data from a single observation space or likelihood). This poses a significant challenge in our setting where different data items can have different likelihoods. [Shon *et al.* \(2006\)](#) proposed a generalisation of the GPLVM model that can handle multiple observation spaces (albeit with Gaussian likelihoods) where the observation spaces are linked by a lower dimensional latent variable space. This was extended by [Ek *et al.* \(2007\)](#) for three-dimensional human pose estimation by incorporating constraints to the latent space. We build upon the idea of obtaining a shared latent space or a common low-dimensional latent representation using a shared GPLVM as proposed in [Ek *et al.* \(2007\)](#). In particular, we extend the idea of shared GPLVM to support multiple likelihoods. Here, the use of non-Gaussian likelihoods introduces intractability into the inference. [Titsias and Lawrence \(2010\)](#) introduced variational inference to the GPLVM assuming the standard Gaussian noise model. However, this model cannot be extended to multiple likelihoods due to the lack of an analytical solution for the optimal variational distribution. We overcome this by using a sampling-based variational inference with numerical integration by Gauss-Hermite quadrature.

Variational inference seeks to approximate the true posterior distribution by minimising the Kullback-Leibler divergence between the true posterior and a surrogate distribution. It can be seen as transforming a complex inference problem into a high-dimensional optimisation problem ([Jordan *et al.*, 1999](#); [Wainwright *et al.*, 2008](#)). [Hoffman *et al.* \(2013\)](#) improved the efficiency of variational inference by proposing an algorithm called stochastic variational inference that incorporated stochastic optimisation into variational inference. To overcome the intractability in our setting, we make use of a variant of stochastic variational inference, called sampling-based variational inference ([Rezende *et al.*, 2014](#); [Kingma and Welling, 2013](#); [Titsias and Lázaro-Gredilla, 2014](#)), and combine that with numerical quadrature. The faster convergence achieved by using mini-batching with the recognition models compensates for the sampling overheads. The introduction of the recognition models brings our method closer to the variational autoencoder. Autoencoders try to learn a latent representation using a neural network to encode the data from the data space to a low-dimensional latent space (encoder) and a separate neural network to decode the data from the

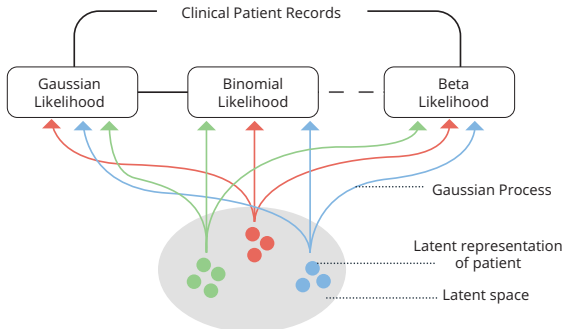


Figure 2: Model overview. Each point in the image corresponds to a patient, whose clinical observations comprise of data from different likelihoods, has been projected on to a two dimensional latent space. The colour coding in the latent space would correspond to disease subtypes.

low-dimensional latent space back to the data space (decoder) (Hinton and Salakhutdinov, 2006). In our approach, the recognition model introduced into the extended GPLVM architecture acts as a form of encoder, while the probabilistic GP mapping acts as a decoder.

Our main contribution in this paper is the extension of the Gaussian process latent variable models (GPLVMs) to produce low-dimensional embeddings of heterogeneous datasets while preserving the similarities between the observations. In other words, our method is a non-linear dimensionality reduction technique intended for heterogeneous data. The key principle in our model is to use the outputs of latent Gaussian processes to modulate the parameters of the different likelihoods through the use of link functions. Our model makes use of the inducing variable formalism for GPLVMs introduced in Titsias and Lawrence (2010). We derive a variational lower bound (ELBO) that makes use of numerical quadrature and is suitable for stochastic optimisation as in Gal *et al.* (2015). Also, we make use of the idea of back-constraints to parameterise the variational inference and encourage distant points in the data space to be distant in the latent space while preserving local similarities (Lawrence and Quiñero-Candela, 2006). The use of back-constraints through a recognition model allows our method to scale to larger datasets by allowing the use of mini-batching (Bui and Turner, 2015). We demonstrate the applicability of our proposed method on clinical data of patients treated for Parkinson’s disease at the HUS Helsinki University Hospital. Fig. 2 illustrates our study’s objective.

In Sec. 2, we discuss our method in detail. The results of our analysis on the Parkinson’s dataset as well as

a detailed description of the dataset can be found in Sec. 3. In Sec. 4, we conclude our paper with a discussion of the results and possible avenues for future research.

2 Methods

Consider a generative model for a dataset $\mathbf{Y} = (\mathbf{y}_1, \dots, \mathbf{y}_N)^T$ with N observations (or patients in our case) and D variables of possibly different observation spaces (or as in our case, patient records from several disparate sources). The dataset can be represented by a set of output functions $\mathcal{Y} = \{y_d(\mathbf{x}_n)\}_{d=1}^D$, where $\mathbf{x}_n \in \mathbb{R}^Q$ is the Q dimensional latent space representation for the n^{th} observation $\forall n = 1, \dots, N$. Every observation (row) in \mathbf{Y} can be represented by a Q dimensional \mathbf{x} , and collectively \mathbf{Y} can be represented by $\mathbf{X} = (\mathbf{x}_1, \dots, \mathbf{x}_N)^T \in \mathbb{R}^{N \times Q}$. The traditional GPLVM model considers the case where $y_d(\mathbf{x})$ is Gaussian distributed (Lawrence, 2004). Wu *et al.* (2017) and Gal *et al.* (2015) have proposed modifications to the GPLVM for Poisson and categorical data, respectively. Similarly, in the supervised learning setting, Moreno-Muñoz *et al.* (2018) proposed an extension of the multi-output Gaussian process regression that can handle heterogeneous outputs. In this paper, we propose a shared GPLVM (Ek *et al.*, 2007) approach for which data items in \mathbf{Y} may be differently distributed following Gaussian, binary, beta, Poisson or categorical distributions. We assume that the likelihood for the d^{th} variable, $y_d(\mathbf{x}_n)$, is specified by a set of parameters $\boldsymbol{\vartheta}_d(\mathbf{x}_n) = [\vartheta_{d,1}(\mathbf{x}_n), \dots, \vartheta_{d,P_d}(\mathbf{x}_n)] \in \psi^{P_d}$, where P_d is the number of parameters that define the distribution and ψ is a generic domain for the parameters. We can think of each element $\vartheta_{d,p}(\mathbf{x}_n)$ of parameter vector $\boldsymbol{\vartheta}_d(\mathbf{x}_n)$ as a non-linear transformation of a Gaussian process prior $\mathcal{F}_{d,p}$, such that $\vartheta_{d,p}(\mathbf{x}_n) = \phi_{d,p}(\mathcal{F}_{d,p}(\mathbf{x}_n))$ where $\phi_{d,p}(\cdot)$ acts as a link function (deterministic function) that maps the GP output to the appropriate domain for the parameter $\vartheta_{d,p}$.

To complete the generative model, we assign a Gaussian distribution prior with standard deviation σ_x^2 for the latent variables $\mathbf{x}_n = (x_{n,1}, \dots, x_{n,Q})^T$. The model can be described by the following equations:

$$x_{n,q} \stackrel{\text{iid}}{\sim} \mathcal{N}(0, \sigma_x^2) \quad (1)$$

$$\mathcal{F}_{d,p} \stackrel{\text{iid}}{\sim} \mathcal{GP}(0, k_d(\cdot)) \quad (2)$$

$$f_{n,d,p} = \mathcal{F}_{d,p}(\mathbf{x}_n) \quad (3)$$

$$\vartheta_{d,p}(\mathbf{x}_n) = \phi_{d,p}(f_{n,d,p}) \quad (4)$$

$$y_{n,d} \sim p(\cdot | \boldsymbol{\vartheta}_d(\mathbf{x}_n)), \quad (5)$$

where $n \in \{1, \dots, N\}$, $q \in \{1, \dots, Q\}$, $d \in \{1, \dots, D\}$, $p \in \{1, \dots, P_d\}$, $k_d(\cdot)$ is the GP kernel function, and

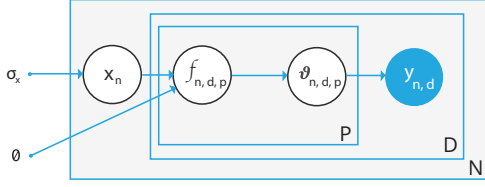


Figure 3: Plate diagram of the model. N , D and P corresponds to the number of observations, variables and parameters respectively. The shaded circle refers to an observed variable and the un-shaded circles corresponds to un-observed variables.

$p(\cdot|\boldsymbol{\vartheta}_d(\mathbf{x}))$ denotes a generic likelihood function for the d^{th} variable. Our model uses the automatic relevance determination radial basis function as the kernel function.

To make the notation concrete, let us consider a case where each observation is comprised of two likelihoods and $D = 4$. Let the first two variables be Gaussian distributed and the last two correspond to count data which we assume to follow a Poisson distribution. In other words, $\mathcal{Y} = \{y_1(\mathbf{x}), y_2(\mathbf{x}), y_3(\mathbf{x}), y_4(\mathbf{x})\}$ where $y_1(\mathbf{x})$ and $y_2(\mathbf{x})$ are Gaussian distributed and $y_3(\mathbf{x})$ and $y_4(\mathbf{x})$ are Poisson distributed. We can say that $y_1(\mathbf{x})$ is modelled by two sets of parameters ($P_1 = 2$), $\boldsymbol{\vartheta}_1(\mathbf{x}) = [\vartheta_{1,1}(\mathbf{x}) \ \vartheta_{1,2}(\mathbf{x})]$ corresponding to the mean and variance, which are functions of \mathbf{x} respectively. We can re-write this as $\boldsymbol{\vartheta}_1(\mathbf{x}) = [\phi_{1,1}(\mathcal{F}_{1,1}(\mathbf{x})) \ \phi_{1,2}(\mathcal{F}_{1,2}(\mathbf{x}))]$ where $\phi_{1,1}(\cdot)$ would be the identity function and $\phi_{1,2}(\cdot)$ could be the exponential function to ensure that variance takes strictly positive values. Likewise, $y_2(\mathbf{x})$ would have a similar formulation. On the other hand, $y_3(\mathbf{x})$ and $y_4(\mathbf{x})$ would be modelled by the Poisson distribution which uses a single parameter ($P_3 = 1$) corresponding to the event rate (also written as λ). The outputs of $y_3(\mathbf{x})$ and $y_4(\mathbf{x})$ correspond to count variables that can take values, $y_3(\mathbf{x}), y_4(\mathbf{x}) \in \mathbb{N} \cup \{0\}$. Considering just $y_3(\mathbf{x})$ for now, we can say that it is modelled by $\boldsymbol{\vartheta}_3 = \vartheta_{3,1}(\mathbf{x}) = \phi_{3,1}(\mathcal{F}_{3,1}(\mathbf{x}))$. The rate parameter is restricted to positive real numbers, hence $\phi_{3,1}(\cdot)$ can be modelled by the exponential function that maps $\exp : \mathbb{R} \rightarrow (0, \infty)$. Likewise, $y_4(\mathbf{x})$ would have a similar formulation.

For our model, we assume that the outputs are conditionally independent given the vector of parameters denoted by $\boldsymbol{\vartheta}(\mathbf{x}) = [\boldsymbol{\vartheta}_1(\mathbf{x}), \boldsymbol{\vartheta}_2(\mathbf{x}), \boldsymbol{\vartheta}_3(\mathbf{x}), \dots, \boldsymbol{\vartheta}_D(\mathbf{x})]$. Hence, the composite likelihood can be defined as

$$p(\mathbf{y}(\mathbf{x})|\boldsymbol{\vartheta}(\mathbf{x})) = p(\mathbf{y}(\mathbf{x})|\mathbf{f}(\mathbf{x})) = \prod_{d=1}^D p(y_d(\mathbf{x})|\boldsymbol{\vartheta}_d(\mathbf{x})),$$

where \mathbf{f} contains realisations of all the GPs from

Eq. (3). Previous works assume that all the variables are from the same observation space. In other words, a homogeneous dataset was represented by a single likelihood. We generalise the GPLVM model to $D \geq 1$ with possibly different likelihoods, thereby allowing it to create low-dimensional representations of heterogeneous datasets (or data from different observation spaces) that are represented by several different likelihoods while capturing the similarities between the observations.

2.1 Likelihood models

We consider the cases of Gaussian, binomial, beta, Poisson and categorical distributions in our analysis. Our model can be easily extended to other distributions as well.

2.1.1 Gaussian distribution

For the Gaussian distribution, the distribution is specified by two parameters: mean and variance. The mean for each data point is obtained from the GPs, while the variance is a shared parameter that is optimised (and constrained to a positive value) to minimise the computational overhead. For the d^{th} measured variable this can be written as $\boldsymbol{\vartheta}_d = [\vartheta_{d,1}(\mathbf{x})]$ where $\vartheta_{d,1}(\mathbf{x})$ is the mean. Therefore, the mean is given by $\vartheta_{d,1}(\mathbf{x}) = \phi_{d,1}(\mathcal{F}_{d,1}(\mathbf{x}))$ where we choose $\phi_{d,1}(\cdot)$ to be the identity function.

2.1.2 Binomial distribution

A binomial distributions is specified by two parameters: number of trials and probability of success in each trial. In our case, for each data point the number of trials is 1. Hence, this can be considered as a Bernoulli trial. We can write $\vartheta_{d,1}(\mathbf{x})$ as the probability of success for the d^{th} variable such that $\boldsymbol{\vartheta}_d = [\vartheta_{d,1}(\mathbf{x})]$. The probability of success would be given by $\vartheta_{d,1}(\mathbf{x}) = \phi_{d,1}(\mathcal{F}_{d,1}(\mathbf{x}))$ where we choose $\phi_{d,1}(\cdot)$ to be the *sigmoid* function (or *softmax* if considering success and failure separately).

2.1.3 Beta distribution

We re-parameterise the beta distribution in terms of mean, μ . Therefore, the two positive shape parameters (α and β) can be written as:

$$\alpha = \nu\mu \quad \text{and} \quad \beta = \nu(1 - \mu),$$

where ν is the inverse dispersion parameter which is a shared parameter that is optimised (and constrained to a positive value). Similar to the previous distributions, μ for each data point is given by $\vartheta_{d,1}(\mathbf{x}) = \phi_{d,1}(\mathcal{F}_{d,1}(\mathbf{x}))$ where we choose $\phi_{d,1}(\cdot)$ to

be the CDF of the standard normal distribution (i.e. $\phi_{d,1}(\mathcal{F}_{d,1}(\mathbf{x})) = \Phi(\mathcal{F}_{d,1}(\mathbf{x}))$).

2.1.4 Poisson distribution

The Poisson distribution is specified by a single positive parameter known as the rate parameter (λ). Similar to the previous distributions, λ for each data point is given by $\vartheta_{d,1}(\mathbf{x}) = \phi_{d,1}(\mathcal{F}_{d,1}(\mathbf{x}))$ where we choose $\phi_{d,1}(\cdot)$ to be the exponential function.

2.1.5 Categorical distribution

For the categorical distribution, we make of a formulation similar to Gal *et al.* (2015) which is a generalisation of the binomial distribution. In this case, the GPs produce the weights for each of the categories. We then make use of the *softmax* function to get probabilities for the categories in the range of $[0, 1]$. Assume all categorical variables to have the same cardinality, K . Hence, $P_d = K$. For the d^{th} variable of the n^{th} entry, we can write $\bar{f}_{n,d} = \{f_{n,d,1}, f_{n,d,2}, \dots, f_{n,d,K}\}$. Following a similar notation to Gal *et al.* (2015), we can write $y_{n,d} \sim \text{softmax}(\bar{f}_{n,d})$, where

$$\text{softmax}(y_{n,d} = k; \bar{f}_{n,d}) = \text{categorical} \left(\frac{\exp(f_{n,d,k})}{\sum_{k'=1}^K \exp(f_{n,d,k'})} \right),$$

and categorical corresponds to the categorical distribution (or generalised Bernoulli distribution).

2.2 Auxiliary variables

The computational complexity of the Gaussian process models is reduced by the introduction of auxiliary variables or inducing inputs (Titsias, 2009). We consider a set of M inducing inputs, $\mathbf{Z} = (\mathbf{z}_1, \dots, \mathbf{z}_M)^T \in \mathbb{R}^{M \times Q}$ that lie in the Q dimensional latent space. Their corresponding outputs in the input space would be $\mathbf{U} = (\mathbf{u}_1, \dots, \mathbf{u}_D) \in \mathbb{R}^{M \times D}$. According to Quiñero-Candela and Rasmussen (2005), the auxiliary variables act as a support for the covariance function of the GP thereby allowing it to be evaluated on these points instead of the entire dataset. Hence, we can perform approximate inference in a time complexity of $\mathcal{O}(M^2N)$ instead of $\mathcal{O}(N^3)$ by evaluating the covariance function of the GP on the auxiliary variables instead of the entire dataset. Continuing the model description, we can write $u_{m,d} = \mathcal{F}_{d,p}(\mathbf{z}_m)$. Moreover, the joint distribution of $(\mathbf{f}_d, \mathbf{u}_d)$ is a multi-variate Gaussian distribution $N(0, \mathbf{K}_d([\mathbf{X}, \mathbf{Z}], [\mathbf{X}, \mathbf{Z}]))$. Further marginalising the inducing outputs leads to a joint distribution of the form $\mathbf{f}_d \sim N(0, \mathbf{K}_d(\mathbf{X}, \mathbf{X}))$, $\forall d$ such that $\mathbf{f}_d \in \mathbb{R}^{N \cdot P_d \times 1}$ (note that, except for the categorical distribution, $P_d = 1$). Hence, the marginal likelihood of the data remains unchanged by the introduction of

the auxiliary variables.

2.3 Variational inference

In our model, the marginal log-likelihood is intractable due to the presence of an arbitrary number of non-Gaussian likelihoods. Hence, we make use of variational inference to compute a lower bound of the log-likelihood (ELBO). We consider a mean field approximation for the latent points $q(\mathbf{X})$ and a joint Gaussian distribution for $q(\mathbf{U})$

$$q(\mathbf{U}) = \prod_{d=1}^D \mathcal{N}(\mathbf{u}_d | \boldsymbol{\mu}_d, \boldsymbol{\Sigma}_d) \quad (6)$$

$$q(\mathbf{X}) = \prod_{n=1}^N \prod_{q=1}^Q \mathcal{N}(x_{n,q} | m_{n,i}, s_{n,q}^2). \quad (7)$$

Following Titsias and Lawrence (2010) and Gal *et al.* (2015), we obtain the ELBO (represented as \mathcal{L}) by applying Jensen's inequality with a variational distribution of the latent variables (full derivation can be found in the Supplement),

$$\begin{aligned} \log p(\mathbf{Y}) &= \log \int p(\mathbf{X}) p(\mathbf{U}) p(\mathbf{F} | \mathbf{X}, \mathbf{U}) \\ &\quad \cdot p(\mathbf{Y} | \mathbf{F}) d\mathbf{X} d\mathbf{F} d\mathbf{U} \\ &\geq - \underbrace{\text{KL}(q(\mathbf{X}) || p(\mathbf{X}))}_{\text{KL}_{\mathbf{X}}} - \underbrace{\text{KL}(q(\mathbf{U}) || p(\mathbf{U}))}_{\text{KL}_{\mathbf{U}}} \\ &\quad + \sum_{d=1}^D \int q(\mathbf{X}) q(\mathbf{u}_d) p(\mathbf{f}_d | \mathbf{X}, \mathbf{u}_d) \\ &\quad \cdot \log p(\mathbf{y}_d | \mathbf{f}_d) d\mathbf{X} d\mathbf{f}_d d\mathbf{U} \\ &= \mathcal{L}. \end{aligned} \quad (8)$$

We further marginalise \mathbf{u}_d in the posterior distribution of \mathbf{f}_d to obtain,

$$\begin{aligned} q(\mathbf{f}_d | \mathbf{X}) &= \int p(\mathbf{f}_d | \mathbf{X}, \mathbf{u}_d) q(\mathbf{u}_d) d\mathbf{u}_d \\ &= \mathcal{N}(\mathbf{f}_d | \mathbf{K}_{NM} \mathbf{K}_{MM}^{-1} \boldsymbol{\mu}_d, \mathbf{K}_{NN} \\ &\quad + \mathbf{K}_{NM} \mathbf{K}_{MM}^{-1} (\boldsymbol{\Sigma}_d - \mathbf{K}_{MM}) \mathbf{K}_{MM}^{-1} \mathbf{K}_{NM}^T), \end{aligned} \quad (9)$$

where $\boldsymbol{\mu}_d$ and $\boldsymbol{\Sigma}_d$ are the variational parameters and \mathbf{K}_{NM} is the cross-covariance matrix computed over \mathbf{Z} and \mathbf{X} . Similarly, \mathbf{K}_{MM} as well as \mathbf{K}_{NN} are the kernel matrices computed on \mathbf{Z} and \mathbf{X} respectively. Using Eq. (9), we can write Eq. (8) as:

$$\begin{aligned} \mathcal{L} &= -\text{KL}_{\mathbf{X}} - \text{KL}_{\mathbf{U}} \\ &\quad + \sum_{d=1}^D \int q(\mathbf{X}) q(\mathbf{f}_d | \mathbf{X}) \log p(\mathbf{y}_d | \mathbf{f}_d) d\mathbf{X} d\mathbf{f}_d. \end{aligned} \quad (10)$$

To solve the integral over \mathbf{X} , we make use of Monte Carlo integration by drawing samples, \mathbf{X}_i from $q(\mathbf{X})$. Hence from Eq. (10), we can write the lower bound \mathcal{L} as:

$$\begin{aligned} \mathcal{L} &\approx -\text{KL}_{\mathbf{X}} - \text{KL}_U \\ &+ \frac{1}{N_x} \sum_{i=1}^{N_x} \sum_{d=1}^D \mathbb{E}_{q(\mathbf{f}_d|\mathbf{X}_i)} [\log p(\mathbf{y}_d|\mathbf{f}_d)], \end{aligned} \quad (11)$$

where N_x corresponds to the number of samples drawn.

2.4 Numerical quadrature

The variational expectation over the log-likelihood, $\log p(\mathbf{y}_d|\mathbf{f}_d)$ in Eq. (11) is intractable. We solve this by making use of the Gauss-Hermite quadrature (Liu and Pierce, 1994). Hence, we follow a sampling-based approach (Kingma and Welling, 2013; Titsias and Lázaro-Gredilla, 2014; Rezende *et al.*, 2014; Hensman *et al.*, 2015) to compute the lower bound \mathcal{L} as well as its derivatives with Gauss-Hermite quadrature. Concretely, we transform the random variables to be sampled using the re-parameterisation trick introduced in Kingma and Welling (2013). The transformation for (vectorised) \mathbf{X} is as follows:

$$\mathbf{X}_i = \mathbf{m} + \mathbf{s}\boldsymbol{\epsilon}_i^{(x)}, \quad \boldsymbol{\epsilon}_i^{(x)} \sim \mathcal{N}(0, I_{N \cdot Q}),$$

where \mathbf{m} and \mathbf{s} contain the variational parameters from Eq. (6). For the quadrature approximation of the expectation with respect to the GPLVM mapping, \mathbf{f}_d (where $\mathbf{f}_d \in \mathbb{R}^{N \cdot P_d \times 1}$) can be transformed as

$$\mathbf{f}_d^{(j)} = \mathbf{a}_d + \mathbf{b}_d t_j,$$

where t_j is the j^{th} zero of the J^{th} order Hermite polynomial as specified by the Gauss-Hermite quadrature and \mathbf{a}_d as well as \mathbf{b}_d are specified from Eq. (9):

$$\begin{aligned} \mathbf{a}_d &= \mathbf{K}_{NM} \mathbf{K}_{MM}^{-1} \boldsymbol{\mu}_d \\ \mathbf{b}_d &= \sqrt{\text{diag}(\mathbf{K}_d)} \\ \mathbf{K}_d &= \mathbf{K}_{NN} + \mathbf{K}_{NM} \mathbf{K}_{MM}^{-1} (\boldsymbol{\Sigma}_d - \mathbf{K}_{MM}) \mathbf{K}_{MM}^{-1} \mathbf{K}_{NM}^T, \end{aligned}$$

where $\text{diag}(\cdot)$ forms a diagonal matrix by setting all non-diagonal elements to zero and $\sqrt{\cdot}$ is element-wise (for diagonal elements).

Hence, we can approximate the expectation for the log-likelihood as a sum of $N \cdot P_d$ one-dimensional numerical quadratures,

$$\begin{aligned} \mathbb{E}_{q(\mathbf{f}_d|\mathbf{X})} [\log p(\mathbf{y}_d|\mathbf{f}_d)] &\approx \\ \sum_{n=1}^N \sum_{j=1}^J \sum_{p=1}^{P_d} w_j q(f_{n,d,p}^{(j)}|\mathbf{X}) &\log p(\mathbf{y}_{n,d}|\mathbf{f}_{n,d,p}^{(j)}), \end{aligned} \quad (12)$$

where $f_{n,d,p}^{(j)}$ indexes the $N \cdot P_d$ elements of $\mathbf{f}_d^{(j)}$, and in our case, we take $J = 3$ making Eq. (12) a 3-point Gauss-Hermite quadrature and w_j are the suitably corresponding weights.

2.5 Variational recognition models

In the standard GPLVM model, there is no constraint that prevents two points which are close in data space to be embedded far apart in latent space (Lawrence and Quiñero-Candela, 2006). Moreover, the use of minibatch-based stochastic variational inference can be impractical for modest size datasets as achieving convergence can take a long time. This is because only the local parameters for a minibatch in each iteration are updated and the optimal $q(\mathbf{X})$ found for the other data points is ignored (Bui and Turner, 2015). We borrow ideas from (Bui and Turner, 2015; Lawrence and Quiñero-Candela, 2006; Rezende *et al.*, 2014) and parameterise the mean and covariance of the variational distribution over $q(\mathbf{X})$ using neural network based recognition models. Concretely, the mean and covariance of $q(\mathbf{x}_n)$ are obtained as the output of two feed-forward, multi-layer perceptrons whose weights are trained by stochastic optimisation

$$q(\mathbf{x}_n|\mathbf{y}_n) = \mathcal{N}(\mathbf{x}_n|\mathcal{M}_{\omega_1}(\mathbf{y}_n), R_{\omega_2}(\mathbf{y}_n)^T R_{\omega_2}(\mathbf{y}_n)),$$

where \mathcal{M} is the mean, R is the cholesky factor of the covariance and ω_1 and ω_2 are the network weights. Therefore, $\mathbf{m}_n = \mathcal{M}_{\omega_1}(\mathbf{y}_n)$ and $\mathbf{S}_n = R_{\omega_2}(\mathbf{y}_n)^T R_{\omega_2}(\mathbf{y}_n)$. By parameterising the distribution over the latent variables by a mapping from the observations, we are introducing a constraint that encourages observations that are close in the data space to be close in the latent representation. Moreover, the use of this formulation allows for the efficient use of minibatching, thereby efficient stochastic optimisation. Specifically, the deep neural network weights, ω_1 and ω_2 act as global parameters that enable parameter sharing. Also, updating these parameters with respect to a data point in a minibatch also affects the latent representation of other data points. The gradients of these back-constraint parameters are obtained using the standard back-propagation algorithm. The choice of weight initialisation for the deep neural networks can affect the training of the weights (Sutskever *et al.*, 2013). We make use of the weight initialisation described in Glorot and Bengio (2010) for both the networks.

2.6 Variational lower bound and stochastic optimisation

The lower bound (ELBO) that needs to be optimised is valid across the data observations and hence, can be

written as

$$\begin{aligned} \mathcal{L} = & - \sum_{n=1}^N \sum_{q=1}^Q \text{KL}(q(x_{n,q}) || p(x_{n,q})) \\ & - \sum_{d=1}^D \text{KL}(q(\mathbf{u}_d) || p(\mathbf{u}_d)) \\ & + \frac{1}{N_x} \sum_{i=1}^{N_x} \sum_{d=1}^D \sum_{n=1}^N \sum_{j=1}^J \sum_{p=1}^{P_d} w_j q(f_{n,d,p}^{(j)} | \mathbf{X}_i) \\ & \cdot \log p(\mathbf{y}_{n,d} | f_{n,d,p}^{(j)}). \end{aligned}$$

It is possible that the resulting latent embeddings may not be centred about the origin even after the model seems sufficiently optimised. This can be observed in some of the visualisations of the latent embeddings. Origin-centred latent embeddings can be achieved by leveraging the idea of introducing a hyper-parameter that balances the latent capacity and independence constraints with reconstruction accuracy as described in Higgins *et al.* (2017). In this paper, we shall call this hyper-parameter as η (see Supplement for more information).

We can make use of a suitable stochastic optimisation technique to minimise the ELBO. The parameters we need to optimise include the recognition model weights (ω_1 and ω_2), variational parameters \mathbf{Z} , $\boldsymbol{\mu}_d$, $\boldsymbol{\Sigma}_d$ and the hyper-parameters for the GP. The optimisation is done using the Adam optimiser (Kingma and Ba, 2014). Adam is also an adaptive learning rate method that maintains an exponentially decaying average of past gradients as well as past squared gradients. Our method allows the computation of derivatives using automatic differentiation. We make use of Theano (Theano Development Team, 2016) for the inference implementation and use the code released with (Gal *et al.*, 2015) as a template for our implementation.¹

3 Experiment

We demonstrated our extended GPLVM model by clustering heterogeneous clinical data. The data comprised of demographic information, diagnostic disease classifications, and clinical laboratory tests of patients having Parkinson’s disease treated in the HUS Helsinki University Hospital, Finland. The demographic information consisted of the patient’s sex and the age when the disease was first diagnosed. This was modelled with binomial and Gaussian likelihoods, respectively. The diagnostic information comprised of International

¹The software implementation will be made available upon publication.

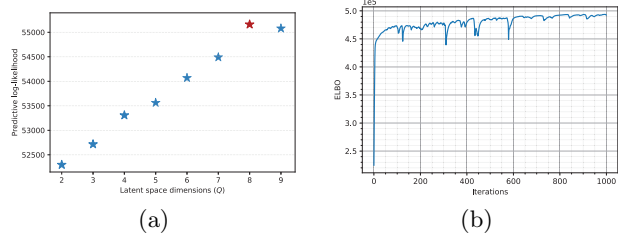


Figure 4: Assessment of optimal latent dimensionality: (a) predictive log-likelihood for different latent space dimensions Q from 7 runs each, and (b) evidence lower bound (ELBO) trajectory during optimisation of the model with $Q = 8$.

Classification of Disease codes (ICD-10) at the categorical level (first three characters) obtained during a five-year follow-up period beginning at six months prior to the first Parkinson’s diagnosis. The disease codes were one-hot encoded into feature vectors and modelled with binomial likelihood. Laboratory measurements from blood (B), erythrocytes (E), plasma (P) or fasting plasma (fP), serum (S), urea (U), and leukocytes (L) (see Figs. 7, 8) were included into feature vectors as the median over the follow-up period. Notably, the laboratory data contained missing values. Variables expressing concentrations and percentages were modelled with Gaussian and beta likelihoods, respectively. Hence, our dataset comprised of approximately 2600 patients with 51-dimensional feature vectors consisting of 20 binomial, 20 Gaussian and 11 beta distributed variables. Also, 10% of the patients were held-out as test data.

First, we assessed the optimal latent dimensionality using the dataset. Fig. 4(a) demonstrates the predicted log-likelihood with test data for different latent dimensionalities. The algorithm was executed seven times per dimensionality and the prediction was done using the model having the largest ELBO over 1000 iterations. Fig. 4(b) shows the ELBO trajectory for the model with $Q = 8$.

Then, we clustered the patient data in the latent space. Based on Fig. 4(a), we selected the model with the highest predictive log-likelihood and made use of the Bayesian Gaussian mixture model to estimate the optimal number of clusters and the cluster membership of each sample (implemented in scikit-learn library (Pedregosa *et al.*, 2011)). The maximum number of clusters was set to 10 and the result with the highest lower bound on the Gaussian mixture model evidence out of 20 initialisations was selected. The final number of clusters was chosen by the algorithm and we excluded clusters containing less than 5% of patients which were subsequently marked as outliers

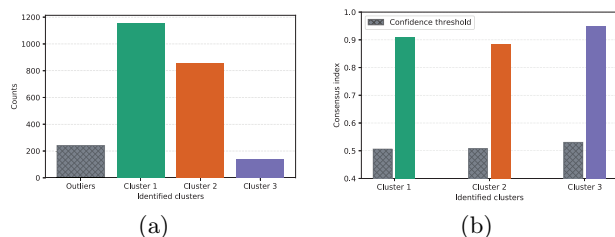


Figure 5: Analysis of the resulting clusters: (a) number of patients in each cluster, and (b) consensus indices, where confidence thresholds indicate Bonferroni corrected 95% percentiles under the null model of no clustering.

(Fig. 5(a)). The resulting clustering was used as a reference in the next step of the analysis.

We performed a robustness analysis for the clustering. Building on the consensus clustering introduced by (Monti *et al.*, 2003), we randomly sub-sampled 50% of the training data, ran the algorithm and applied Gaussian mixture clustering with a fixed number of clusters (previously obtained optimal value). The routine was replicated 91 times. Selecting pairs of two clustering replications, we constructed a $(N \times N)$ consensus matrix, where N is the original number of training samples, and where each element i, j in the matrix represents the (normalised) number of times the two samples occur in the same cluster.

In contrast to matrix reordering and visualisation in (Monti *et al.*, 2003), the previously obtained reference clustering was used for defining the cluster membership of each entry in the consensus matrix. This allowed the computation of the cluster-specific consensus index as the average of the entries (Fig. 5(b)). Moreover, we assessed the consensus indices under a null hypothesis using a permutation test. Here, the cluster membership of samples were randomly re-ordered and consensus indices were computed accordingly. We defined confidence thresholds by computing the 95th percentile over 1000 replications (with Bonferroni correction over clusters). The obtained clusterings for some runs in a two dimensional latent space are visualised in Fig. 3.

Finally, we evaluated the differences in cluster characteristics. We computed logarithmic odds-ratio separately for each binomial variable between the values of samples belonging to a specific cluster and the rest of the data. For other variables, t-statistic was applied. Thus, negative values indicate less frequent occurrence (or smaller values) than the rest of the data, and vice versa. For example, Figs. 7 and 8 indicate that cluster #3 characteristically includes younger people who also have a lower frequency (or smaller value) of diagnoses

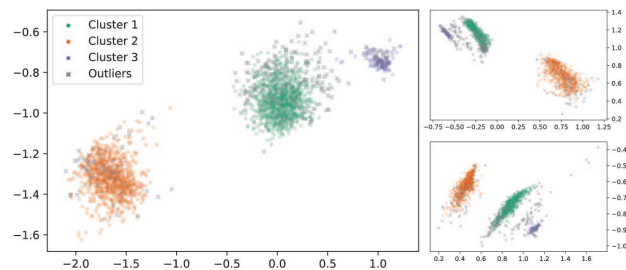


Figure 6: Latent representations of the patients with $Q = 2$ from different runs.

than the rest of the patients in other clusters. In clusters #1 and #2, age is not a determining factor, but the clusters often show opposite characteristics both in prevalence of diagnoses and in laboratory measurements. Altogether, these results demonstrate the feasibility of our approach in finding patient subsets in data-driven manner.

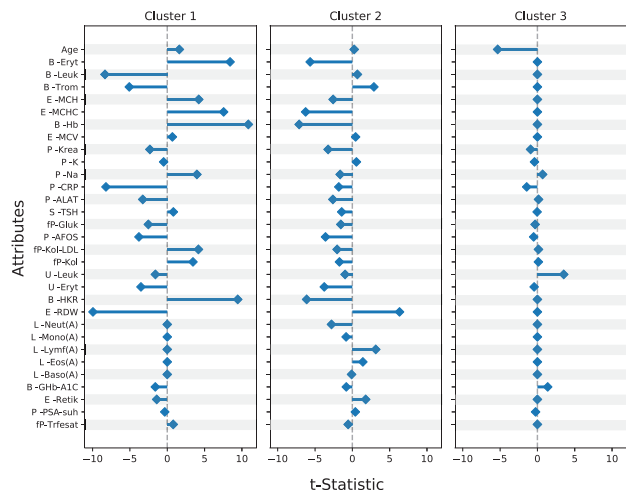


Figure 7: Evaluation of cluster characteristics using t-statistics.

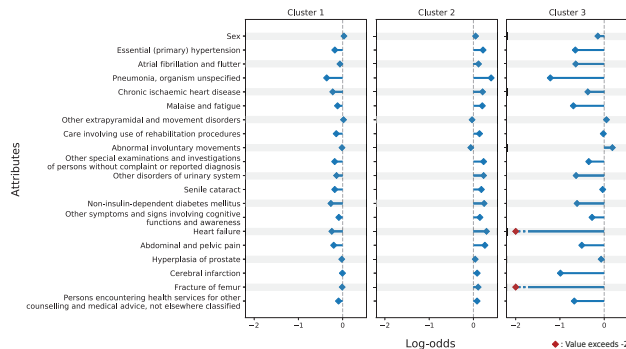


Figure 8: Evaluation of binomial cluster characteristics using log-odds ratio.

From Suppl. Fig. 2, we can observe the relative decrease in the Euclidean distance as the hyperparameter η increases. This shows that incorporating a weight on $\text{KL}_{\mathcal{X}}$ (i.e. $\eta > 1$) results in latent embeddings that are generally centred around the origin with results that are qualitatively consistent with Eq. (11) (i.e. $\eta = 1$).

4 Discussion and Conclusions

This work proposes a generative model that is targeted to clinical datasets that comprise of heterogeneous, high-dimensional data from several disparate sources. We extend the Gaussian process latent variable model (GPLVM) to produce low-dimensional embeddings of heterogeneous datasets while preserving the similarities between the observations by learning a shared latent representation. In this work, we adapt the inference framework proposed in (Titsias and Lawrence, 2010) and back-constrain the latent space using recognition models. We demonstrate the effectiveness of our model on clinical data of Parkinson’s disease patients from the HUS Helsinki University Hospital. Our approach identifies sub-groups from the heterogeneous patient data and we also demonstrate the robustness of the findings. The differences in characteristics among the identified clusters were also evaluated using standard statistical tests. This work ties together many existing models and techniques in the field of generative modelling and demonstrates its effectiveness on clinical data.

We believe that there are many avenues for future research in generative modelling for clinical and biological data. Active learning techniques to incorporate expert knowledge to guide the overall clustering procedure may be of significant interest to clinicians. We also seek to improve our model through better estimation of missing values as sparsity is a significant problem in clinical and biological datasets. Another avenue of future research may be the incorporation of more expressive posterior distributions in the variational inference through the application of flow-based models.

Acknowledgements

We would like to acknowledge the computational resources provided by Aalto Science-IT, Finland. We would also like to thank Gleb Tikhonov and Henrik Mannerström for helpful discussions and comments, Jani Salmi for data preparation, Anu Loukola for project management, and Olli Carpén for discussions and support.

Funding

This work was supported by the Academy of Finland [292660, 313271]; and Business Finland [2383/31/2015].

References

- Achenbach, P., Warncke, K., Reiter, J., Naserke, H. E., Williams, A. J., Bingley, P. J., Bonifacio, E., and Ziegler, A.-G. (2004). Stratification of type 1 diabetes risk on the basis of islet autoantibody characteristics. *Diabetes*, **53**(2), 384–392.
- Ahlqvist, E., Storm, P., Käräjämäki, A., Martinell, M., Dorkhan, M., Carlsson, A., Vikman, P., Prasad, R. B., Aly, D. M., Almgren, P., *et al.* (2018). Novel subgroups of adult-onset diabetes and their association with outcomes: a data-driven cluster analysis of six variables. *The Lancet Diabetes & Endocrinology*, **6**(5), 361–369.
- Bui, T. D. and Turner, R. E. (2015). Stochastic variational inference for gaussian process latent variable models using back constraints. In *Black Box Learning and Inference NIPS workshop*.
- Ek, C. H., Torr, P. H., and Lawrence, N. D. (2007). Gaussian process latent variable models for human pose estimation. In *International workshop on machine learning for multimodal interaction*, pages 132–143. Springer.
- Gal, Y., Chen, Y., and Ghahramani, Z. (2015). Latent gaussian processes for distribution estimation of multivariate categorical data. In *Proceedings of the 32nd International Conference on Machine Learning*.
- Glorot, X. and Bengio, Y. (2010). Understanding the difficulty of training deep feedforward neural networks. In *Proceedings of the thirteenth international conference on artificial intelligence and statistics*, pages 249–256.
- Harvey, A., Brand, A., Holgate, S. T., Kristiansen, L. V., Lehrach, H., Palotie, A., and Prainsack, B. (2012). The future of technologies for personalised medicine. *New biotechnology*, **29**(6), 625–633.
- Hensman, J., Matthews, A., and Ghahramani, Z. (2015). Scalable variational gaussian process classification. *Journal for Machine Learning Research*.
- Higgins, I., Matthey, L., Pal, A., Burgess, C., Glorot, X., Botvinick, M., Mohamed, S., and Lerchner, A. (2017). beta-vae: Learning basic visual concepts with a constrained variational framework. *ICLR*, **2**(5), 6.
- Hinton, G. E. and Salakhutdinov, R. R. (2006). Reducing the dimensionality of data with neural networks. *science*, **313**(5786), 504–507.

- Hoffman, M. D., Blei, D. M., Wang, C., and Paisley, J. (2013). Stochastic variational inference. *The Journal of Machine Learning Research*, **14**(1), 1303–1347.
- Jordan, M. I., Ghahramani, Z., Jaakkola, T. S., and Saul, L. K. (1999). An introduction to variational methods for graphical models. *Machine learning*, **37**(2), 183–233.
- Kalia, L. V. and Lang, A. E. (2015). Parkinson’s disease. *The Lancet*, **386**(9996), 896–912.
- Kingma, D. P. and Ba, J. (2014). Adam: A method for stochastic optimization. *arXiv preprint arXiv:1412.6980*.
- Kingma, D. P. and Welling, M. (2013). Auto-encoding variational bayes. *arXiv preprint arXiv:1312.6114*.
- Lawrence, N. D. (2004). Gaussian process latent variable models for visualisation of high dimensional data. In *Advances in neural information processing systems*, pages 329–336.
- Lawrence, N. D. and Quiñonero-Candela, J. (2006). Local distance preservation in the GP-LVM through back constraints. In *Proceedings of the 23rd international conference on Machine learning*, pages 513–520. ACM.
- Liu, Q. and Pierce, D. A. (1994). A note on gauss-hermite quadrature. *Biometrika*, **81**(3), 624–629.
- Monti, S., Tamayo, P., Mesirov, J., and Golub, T. (2003). Consensus clustering: a resampling-based method for class discovery and visualization of gene expression microarray data. *Machine Learning*, **52**(1–2), 91–118.
- Moreno-Muñoz, P., Artés, A., and Álvarez, M. (2018). Heterogeneous multi-output gaussian process prediction. In S. Bengio, H. Wallach, H. Larochelle, K. Grauman, N. Cesa-Bianchi, and R. Garnett, editors, *Advances in Neural Information Processing Systems 31*, pages 6712–6721. Curran Associates, Inc.
- Pedregosa, F., Varoquaux, G., Gramfort, A., Michel, V., Thirion, B., Grisel, O., Blondel, M., Prettenhofer, P., Weiss, R., Dubourg, V., Vanderplas, J., Passos, A., Cournapeau, D., Brucher, M., Perrot, M., and Duchesnay, E. (2011). Scikit-learn: Machine learning in Python. *Journal of Machine Learning Research*, **12**, 2825–2830.
- Quiñonero-Candela, J. and Rasmussen, C. E. (2005). A unifying view of sparse approximate gaussian process regression. *Journal of Machine Learning Research*, **6**(Dec), 1939–1959.
- Rasmussen, C. E. (2004). Gaussian processes in machine learning. In *Advanced lectures on machine learning*, pages 63–71. Springer.
- Rezende, D. J., Mohamed, S., and Wierstra, D. (2014). Stochastic backpropagation and approximate inference in deep generative models. *arXiv preprint arXiv:1401.4082*.
- Shon, A., Grochow, K., Hertzmann, A., and Rao, R. P. (2006). Learning shared latent structure for image synthesis and robotic imitation. In *Advances in neural information processing systems*, pages 1233–1240.
- Sutskever, I., Martens, J., Dahl, G., and Hinton, G. (2013). On the importance of initialization and momentum in deep learning. In *International conference on machine learning*, pages 1139–1147.
- Theano Development Team (2016). Theano: A Python framework for fast computation of mathematical expressions. *arXiv e-prints*, **abs/1605.02688**.
- Tipping, M. E. and Bishop, C. M. (1999). Probabilistic principal component analysis. *Journal of the Royal Statistical Society*, **61**(3), 611–622.
- Titsias, M. (2009). Variational learning of inducing variables in sparse gaussian processes. In *Artificial Intelligence and Statistics*, pages 567–574.
- Titsias, M. and Lawrence, N. D. (2010). Bayesian gaussian process latent variable model. In *Proceedings of the Thirteenth International Conference on Artificial Intelligence and Statistics*, pages 844–851.
- Titsias, M. and Lázaro-Gredilla, M. (2014). Doubly stochastic variational bayes for non-conjugate inference. In *International Conference on Machine Learning*, pages 1971–1979.
- Wainwright, M. J., Jordan, M. I., et al. (2008). Graphical models, exponential families, and variational inference. *Foundations and Trends® in Machine Learning*, **1**(1–2), 1–305.
- Wu, A., Roy, N. G., Keeley, S., and Pillow, J. W. (2017). Gaussian process based nonlinear latent structure discovery in multivariate spike train data. In *Advances in Neural Information Processing Systems*, pages 3496–3505.

Latent Gaussian process with composite likelihoods for data-driven disease stratification

Supplement

1 Derivation of the evidence lower bound (ELBO)

To obtain the ELBO, we can first write the log-likelihood as,

$$\log p(\mathbf{Y}) = \log \int p(\mathbf{X})p(\mathbf{U})p(\mathbf{F}|\mathbf{X}, \mathbf{U})p(\mathbf{Y}|\mathbf{F})d\mathbf{X}d\mathbf{F}d\mathbf{U}.$$

Multiplying and dividing by $q(\mathbf{X}, \mathbf{F}, \mathbf{U})$, we can re-write the log-likelihood as,

$$\log p(\mathbf{Y}) = \log \int \frac{q(\mathbf{X}, \mathbf{F}, \mathbf{U})}{q(\mathbf{X}, \mathbf{F}, \mathbf{U})} p(\mathbf{X})p(\mathbf{U})p(\mathbf{F}|\mathbf{X}, \mathbf{U})p(\mathbf{Y}|\mathbf{F})d\mathbf{X}d\mathbf{F}d\mathbf{U}. \quad (1)$$

The variational approximation to the posterior distribution, $q(\mathbf{X}, \mathbf{F}, \mathbf{U})$, can be factorised as follows:

$$q(\mathbf{X}, \mathbf{F}, \mathbf{U}) = q(\mathbf{X})q(\mathbf{U})p(\mathbf{F}|\mathbf{X}, \mathbf{U}). \quad (2)$$

Substituting into Eq. (1), we get:

$$\begin{aligned} \log p(\mathbf{Y}) = \log \int & q(\mathbf{X})q(\mathbf{U})p(\mathbf{F}|\mathbf{X}, \mathbf{U}) \\ & \cdot \frac{p(\mathbf{X})p(\mathbf{U})p(\mathbf{F}|\mathbf{X}, \mathbf{U})p(\mathbf{Y}|\mathbf{F})}{q(\mathbf{X})q(\mathbf{U})p(\mathbf{F}|\mathbf{X}, \mathbf{U})} d\mathbf{X}d\mathbf{F}d\mathbf{U}. \end{aligned} \quad (3)$$

Jensen's inequality relates the value of a concave (or convex) function of an integral to the integral of the concave (or convex) function (Jensen *et al.*, 1906). Assume φ is a concave function and X is a random variable. By the Jensen's inequality for a concave function, we can write:

$$\varphi(\mathbb{E}[X]) \geq \mathbb{E}[\varphi(X)]. \quad (4)$$

In our model, we have $\varphi = \log$. Substituting this in Eq. (4) and for a random variable X , we have:

$$\log(\mathbb{E}[X]) \geq \mathbb{E}[\log(X)]. \quad (5)$$

We can now apply the Jensen’s inequality from Eq. (5) to Eq. (3):

$$\begin{aligned} \log p(\mathbf{Y}) &\geq \int q(\mathbf{X})p(\mathbf{U})p(\mathbf{F}|\mathbf{X}, \mathbf{U}) \\ &\cdot \log \frac{p(\mathbf{X})p(\mathbf{U})p(\mathbf{F}|\mathbf{X}, \mathbf{U})p(\mathbf{Y}|\mathbf{F})}{q(\mathbf{X})p(\mathbf{U})p(\mathbf{F}|\mathbf{X}, \mathbf{U})} d\mathbf{X}d\mathbf{F}d\mathbf{U}. \end{aligned} \quad (6)$$

The Kullback-Leibler divergence (Kullback and Leibler, 1951) between $q(\mathbf{X})$ and $p(\mathbf{X})$ as well as between $q(\mathbf{U})$ and $p(\mathbf{U})$ can be written as

$$\begin{aligned} \text{KL}(q(\mathbf{X})||p(\mathbf{X})) &= \int q(\mathbf{X}) \log \frac{q(\mathbf{X})}{p(\mathbf{X})} d\mathbf{X}, \\ \text{KL}(q(\mathbf{U})||p(\mathbf{U})) &= \int q(\mathbf{U}) \log \frac{q(\mathbf{U})}{p(\mathbf{U})} d\mathbf{U}. \end{aligned}$$

Substituting the KL divergences in Eq. (6) and unwrapping the remaining terms along the dimension d (i.e. the dimension of the data space) from their vectorised form, we get:

$$\begin{aligned} \log p(\mathbf{Y}) &\geq -\text{KL}(q(\mathbf{X})||p(\mathbf{X})) - \text{KL}(q(\mathbf{U})||p(\mathbf{U})) \\ &+ \sum_{d=1}^D \int q(\mathbf{X})q(\mathbf{u}_d)p(\mathbf{f}_d|\mathbf{X}, \mathbf{u}_d) \cdot \log p(\mathbf{y}_d|\mathbf{f}_d) d\mathbf{X}d\mathbf{f}_d d\mathbf{u}_d = \mathcal{L}. \end{aligned} \quad (7)$$

2 Origin-centred latent representations

In this paper, we demonstrated that using $\eta > 1$ results in embeddings that are more centred about the origin but with qualitatively consistent results (i.e. qualitatively consistent with the hyper-parameter $\eta = 1$). From Eq. (11) in the main paper, we can write the lower bound \mathcal{L} with our suggested modification as follows:

$$\begin{aligned} \mathcal{L} &\approx -\eta \overbrace{\text{KL}(q(\mathbf{X})||p(\mathbf{X}))}^{\text{KL}_{\mathbf{X}}} - \overbrace{\text{KL}(q(\mathbf{U})||p(\mathbf{U}))}^{\text{KL}_{\mathbf{U}}} \\ &+ \frac{1}{N_x} \sum_{i=1}^{N_x} \sum_{d=1}^D \mathbb{E}_{q(\mathbf{f}_d|\mathbf{x}_i)} [\log p(\mathbf{y}_d|\mathbf{f}_d)], \end{aligned} \quad (8)$$

where η is the new hyper-parameter. If $\eta = 1$, we get the same equation as Eq. (11) in the main paper.

To obtain a centred embedding, the hyper-parameter η must be tuned. We have also observed that as the value of η begins to increase to larger values, the clustering structure begins to disappear as the KL term associated with X (i.e. $\text{KL}_{\mathbf{X}}$ in Eq. (8)) begins to dominate and the optimisation tries to move the latent points closer to zero while making them appear to be a sample from the

standard normal distribution.

Hence, we can infer that incorporating a weight on $\text{KL}_{\mathbf{X}}$ (i.e. $\eta > 1$) results in latent embeddings that are generally centred around the origin with results that are qualitatively consistent with Eq. (11) in the main paper (i.e. $\eta = 1$).

3 Supplementary figures

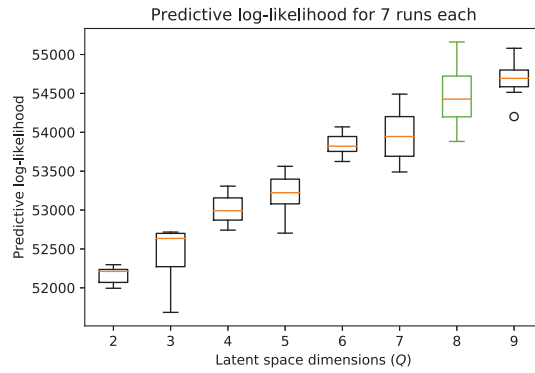


Figure 1: Box plot for the assessment of optimal latent dimensionality

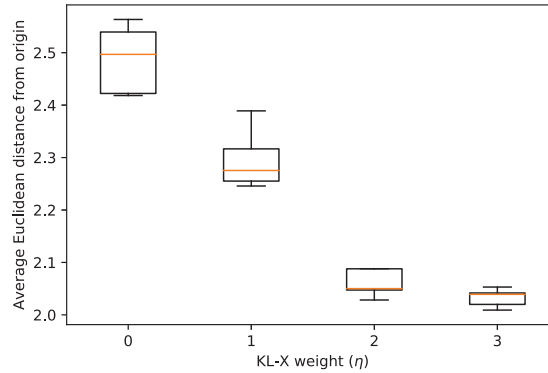


Figure 2: Demonstration of the effect of η using $Q = 8$ with 5 runs each. This is generated from the average Euclidean distance of the latent embeddings from the origin for each run.

References

- Jensen, J. L. W. V. *et al.* (1906). Sur les fonctions convexes et les inégalités entre les valeurs moyennes. *Acta mathematica*, **30**, 175–193.
- Kullback, S. and Leibler, R. A. (1951). On information and sufficiency. *The annals of mathematical statistics*, **22**(1), 79–86.